

# **Wind Farm - Midterm Report**

## **I PRO 344 - FALL 2006**

Advisor: Professor M. Shahidehpour  
Sponsor: Michael Polsky, Invenergy LLC

Team Members:  
Luke Cho  
Euddum Choi  
Sushma Dantapalli  
Sandhya Duggirala  
Bahram Kayvani  
Azim Lotfjou  
Sung Song  
Dan Taulbee  
Michael Urbina  
Jieum Yoo

## Revised Objectives

The objectives for the IPRO 344 project have not changed significantly:

- Selection of several sites, taking into account wind availability, proximity to transmission lines, environmental impact, and the selling price of electricity at the location.
- Mechanical design of the wind turbine, including the blades, turbine, and tower.
- Electrical design of the generator, grid interconnection, and control system.
- A study of the economics of the design, including a life-cycle cost analysis.

It was chosen to focus on several sites, rather than choosing only one. Also, a more extensive market analysis was added to the scheduled tasks to attempt to determine the impact of adding wind turbines on the power system and the power market.

## Results to Date

The IPRO 344 project has completed the following tasks:

- Determined Wind Farm Location
- Completed the Mechanical Design
  - Blade Design
  - Hub Design
  - Generator Type
- Determined the economic value of wind projects at the selected sites
- Studied the impact of adding wind turbines at the selected locations on the power system and the power market

### ***The locations***

The area nearby the cities of Bloomington, Pittsfield and Rochelle in the state of Illinois, and an off-shore location in Lake Michigan, near Chicago, were chosen based on wind resource maps available in [1]. These locations are classified as having a good wind power potential with a wind speed average of 7–7.4 m/s at 50m. In contrast, the average wind speed during the past 5 years, collected from nearby weather stations [2], is somewhat different from the wind resource map, except for the Chicago area. The observations stations are at ground level, however, so the observed wind speed at an assumed hub height of 80m was calculated using [3], assuming a roughness class of zero for the offshore location, and class two for the inland locations. Additionally, since the turbine only operates with wind speeds between 3.5 and 25 m/s, the average percentage of days the turbine operates, referred to in Table 1 as the Operating Days, is calculated, as

well as the average wind speed for these days. A Weibull probability distribution, given by

$$W(x) = \frac{k}{\lambda} \left( \frac{x}{\lambda} \right)^{k-1} e^{-\left( \frac{x}{\lambda} \right)^k} \quad (1)$$

Where,

$W(x)$  = Weibull Distribution function

$x$  = Wind Speed Probability

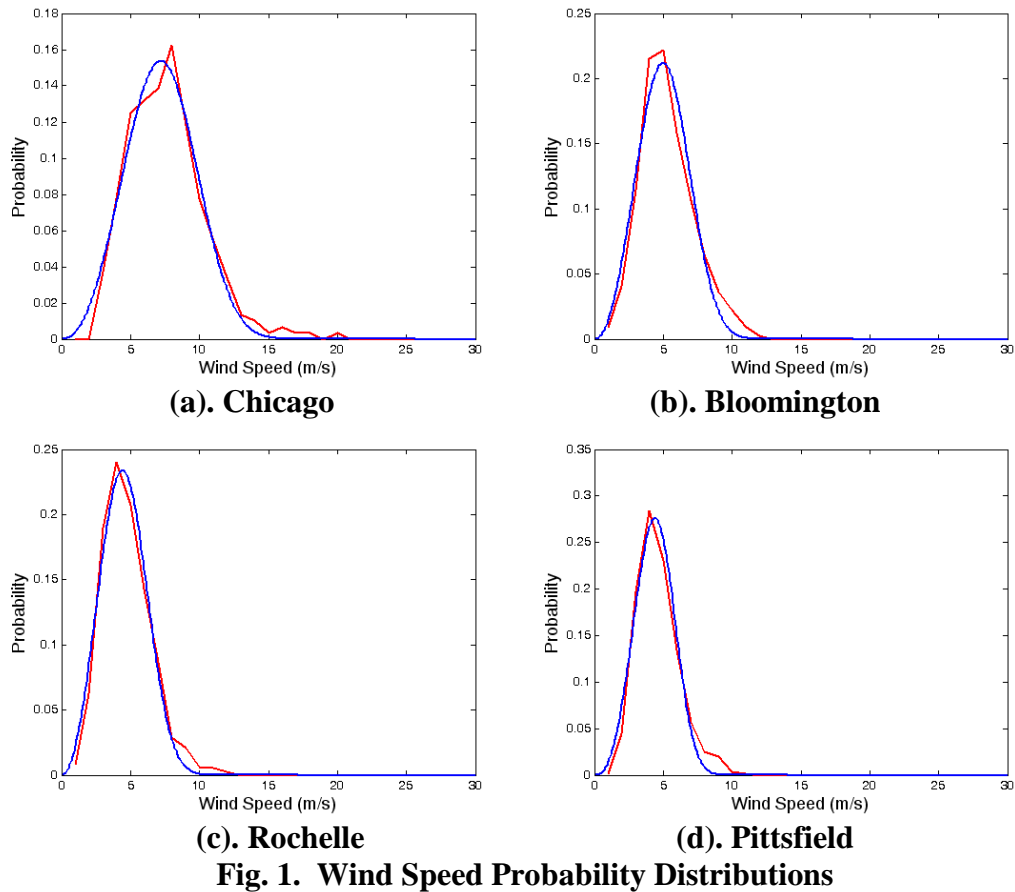
$k$  = Shape Factor

$\lambda$  = Scale Factor

is fitted to the wind distribution for each site by determining the shape and scale parameters, as shown in figures 1a through 1d, where the red line indicates the actual probability distribution, and the blue line represents the fitted Weibull curve. Based on this data, the offshore Chicago location offers by far the greatest potential wind resource of the four locations due to not only high wind speeds, but also a very high percentage of operating days.

**Table I. Wind Speed Data**

Location	Observed Average Wind Speed at 10m (m/s)	Calculated Wind Speed at 80m (m/s)	Operating Wind Speed at 10m (m/s)	Operating Wind Speed at 80m (m/s)	Percentage Operating Days
Chicago	7.12	8.49	7.39	8.81	94%
Bloomington	4.89	7.10	5.626	8.17	76%
Rochelle	3.66	5.55	5.3	7.69	65%
Pittsfield	3.25	4.72	5.19	7.53	66%



## ***Blade Design***

### **Number of Blades**

Commercial wind turbines are designed as single-blade, two-blade and three blade turbines. Apart from the saving in rotor cost itself, the single-blade and two-blade turbine concepts are attractive because of the reduction in drive train cost realizable through increased rotational speed. An obvious disadvantage is the resulting increased noise emission resulting from the faster rotation, but this would not be an issue offshore. Another consideration is the reduced yield due to increased tip between 12 percent and 19 percent in comparison to three-blade turbines.

Although the assessment of visual appearance is essentially subjective, there is an emerging consensus that three-blade machines are more restful to look at than single-blade and two-blade ones. So, with regarding to above reasons, three-blade machines will be considered in designing the wind turbine.

## Blade Size

Because the rotor diameter has the largest single influence on the design and scale of a turbine and most component scaling equations are a function of the rotor diameter, the primary calculations are focused on finding the appropriate rotor size.

Rotor size can be calculated after determining the power curve of the wind turbine. The output power can be expressed according to

$$P_v = P_R \left( \frac{V^n - V_I^n}{V_R^n - V_I^n} \right) \quad (2)$$

where,

- $n$  = velocity-power proportionality
- $V_R$  = rated velocity of the turbine
- $V_I$  = cut-in velocity of the turbine
- $V_o$  = cut-out velocity of the turbine
- $P_R$  = Rated power of the wind turbine

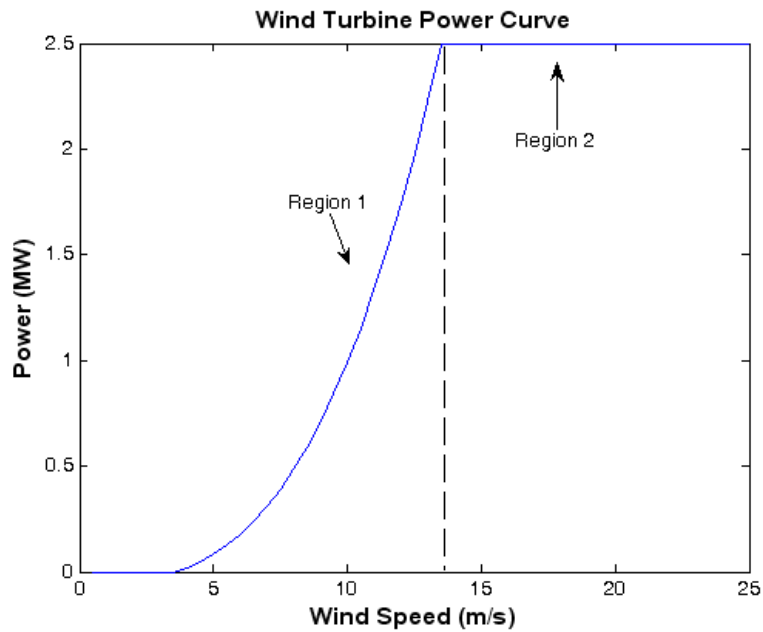


Fig. 2. Wind Turbine Power Curve

For a generator with  $P_R = 2.5\text{MW}$ , to maximize the efficiency ( $\eta_g = 0.9$ ) the parameters are chosen as

$$\begin{aligned} n &= 3 \\ V_R &= 12 \text{ m/s} \\ V_I &= 3.5 \text{ m/s} \\ V_o &= 25 \text{ m/s} \\ P_R &= 2.5 \text{ MW} \end{aligned}$$

The output power with respect to various wind speeds is approximated, as in Fig. 2, by two regions. The energy generated by the turbine in each region is obtained using the following relations

$$E_{1R} = \frac{P_R T}{V_R^n - V_I^n} \int_{V_I}^{V_R} (V^n - V_I^n) \frac{k}{c} \left(\frac{V}{c}\right)^{k-1} e^{-\left(\frac{V}{c}\right)^k} dV \quad (3)$$

$$E_{R0} = P_R T \int_{V_R}^{V_o} \frac{k}{c} \left(\frac{V}{c}\right)^{k-1} e^{-\left(\frac{V}{c}\right)^k} dV \quad (4)$$

$$E_T = E_{1R} + E_{R0} \quad (5)$$

where,

$$\begin{aligned} E_{1R} &= \text{energy for wind speeds in region 1} \\ E_{R0} &= \text{energy for wind speeds in region 2} \\ E_T &= \text{total energy} \end{aligned}$$

Matching the wind turbine design with the wind resource at a given location is crucial when planning. The amount of energy generated results in revenues and therefore it has to be maximized, while the dimensions and other characteristics of the design are still feasible. The capacity factor is a widely used index, and here it is used to measure if the wind turbine design is appropriate to the wind distribution curve at the chosen locations. For this purpose, we look for a design that has a capacity factor bigger than 0.25 as shows the following equation.

$$C_F = \frac{E_T}{T \times P_R} > 0.25 \quad (6)$$

The rotor radius depends primarily on the power expected from the turbine and the average wind speed at the site. Equation (7) represents the relationship of the rotor radius and other parameters.



where,

$T$  = temperature ( $^{\circ}\text{C}$ )

$c_0 = 0.99999683$

$c_1 = -0.90826951\text{e-}2$

$c_2 = 0.78736169\text{e-}4$

$c_3 = -0.61117958\text{e-}6$

$c_4 = 0.43884187\text{e-}8$

$c_5 = -0.29883885\text{e-}10$

$c_6 = 0.21874425\text{e-}12$

$c_7 = -0.17892321\text{e-}14$

$c_8 = 0.11112018\text{e-}16$

$c_9 = -0.30994571\text{e-}18$

Based on the above calculations, the optimal blade radius for each site was calculated to be approximately 45m, as shown below in table II.

**Table II. Theoretical rotor radius**

Location	k	c	Ea	CF	R (m)
Chicago	3.14	15.35	15795.78	0.72	44.97
Bloomington	2.99	10.51	8864.41	0.40	43.91
Rochelle	2.91	9.29	6580.34	0.30	45.58
Pittsfield	3.37	8.89	5634.06	0.26	44.40

## Blade Geometry

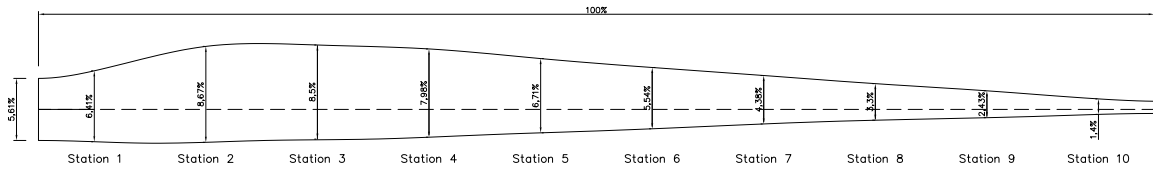


**Fig. 3. Preliminary Blade Design**

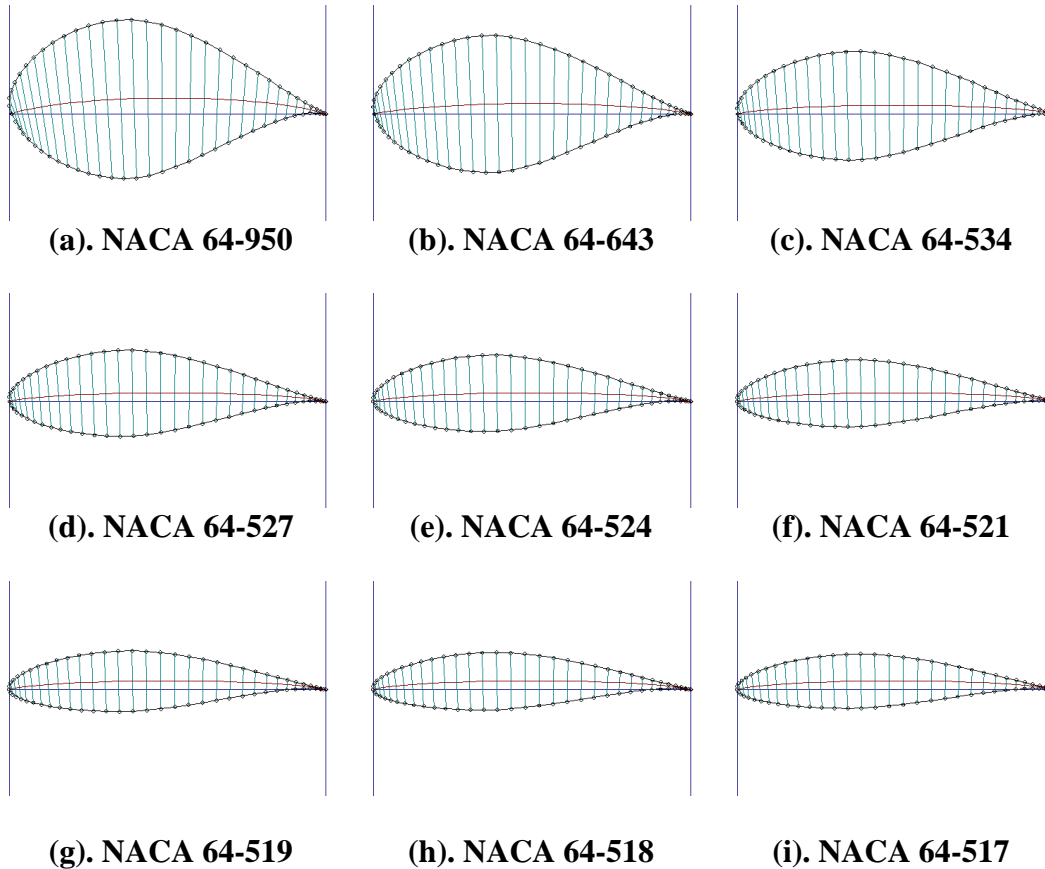


**Fig. 4. Blade Cross Sections**

The design process of a blade geometry started with a baseline planform shown in Fig. 3. The planform is divided in 10 sections, or stations as shown in Fig 4. Each station is characterized by a different chord width, thickness, setting angle and airfoil profile. In order to determine the design lift coefficient of the station profile and the respective setting angle the relationships shown in equations (11) and (12) were used.

$$\phi = \frac{2}{3} \times \tan^{-1} \left( \frac{1}{\lambda_D \times r} \right) - \alpha \quad (11)$$

where,

- $\phi$  = Blade setting angle (degrees)
- $\lambda_D$  = Design tip speed ratio
- $r$  = Radius ratio (%)
- $\alpha$  = Angle of attack (degrees)

$$c_{LD} = \frac{8 \times \pi \times r \times R}{B \times C} \quad (12)$$

where,

- $c_{LD}$  = Design lift coefficient
- $C$  = Chord width
- $B$  = Number of blades

For wind power applications, the airfoil profile of each section must have a high lift to drag coefficient ratio [6]. Here we choose the NACA 6 Aerofoil Series to compose the blade sections because its geometry has high lift to drag coefficient ratio [7]. The lift to drag coefficients of NACA 6 Aerofoil Series were investigated, and in average the appropriate angle of attack for wind turbine applications is 4 degrees.

Note that here we fix the chord width and calculate the design lift coefficient. Usually the chord width is calculated for a fixed design lift coefficient. In a preliminary study, we chose the NACA 63-415 and used this approach. The blade width results were too large close the hub and too thin close to the blade tip. Large-scale wind turbines required different design lift coefficient and therefore different airfoil profiles along the blade length.

Then, the next steps are to chose the appropriate airfoils and verify their lift to drag coefficient ratio. In order to accomplish this verification, we use the airfoil simulation software DesignFOIL. A good design must have a lift to drag coefficient ratio of 110-130 for a Reynolds Number of 3 million [7].

Because the optimal blade radius for all locations was very close to 45m, a single blade was designed for all locations, as specified in table III. The complete design is given in the appendix.

**Table III. Blade Specifications**

Station Number	Radius Length (m)	Chord Width (m)	Blade Thickness (m)
1	2.25	2.88	2.45
2	6.75	3.9	2.06
3	11.25	3.88	1.89
4	15.75	3.59	1.27
5	20.25	3.02	0.84
6	24.75	2.49	0.51
7	29.25	1.97	0.43
8	33.75	1.49	0.3
9	38.25	1.09	0.23
10	42.75	0.83	0.14

o realize 3-dimension design of wind turbine based on the 2-dimension design of cad, it is necessary to be familiar with 3-D function of Cad and rendering of max program. First of all, we've already got 2-D design of a rotor blade. So the first goal is to realize 3-D of a rotor blade design. Because of rotor blade have different cross sections according on one of blades; it needs to overlap several cross sections and building up with Extrude function of Cad to realize 3-D. But the problem is it is hard to get center point of each cross section and to connect all boundaries through wires to be seemed as a real material. Therefore, it will take a couple of days to figure out these problems. And after finishing 3-D design of blades, we will try to rendering of 3-D design with Max program. Through rendering, we can perfectly visualize and simulation of the blade design.

## **Generator**

Generators consist of two types - those that operate synchronously with the AC frequency of the electric grid, and induction generators, which operate asynchronously. Traditional generators are powered by a directly controllable energy source, such as coal or nuclear energy, so the input torque and speed of rotation can be set as needed. For these applications, synchronous generators are most common. For wind power, however, the input torque is highly variable and unpredictable. Although the generator torque can be controlled to some degree by changing the pitch of the blades, this control may be insufficient, therefore, asynchronous generators are often required.

## Synchronous Generator

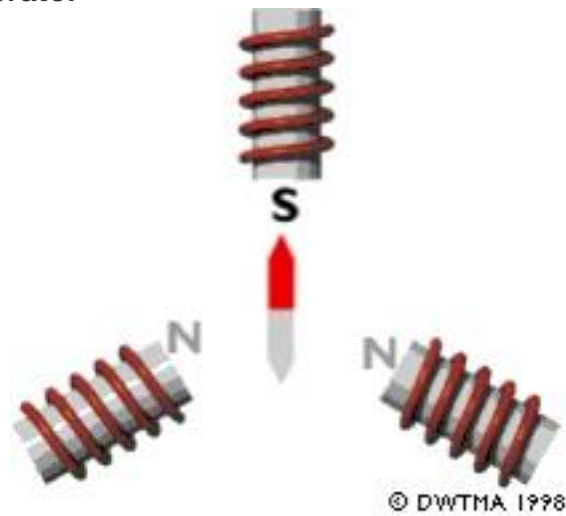


**Fig. 5. Synchronous Generator**

The synchronous generator operates at a constant angular velocity that is synchronized to the AC frequency of the electrical grid. It is the most common choice for power generation applications due to the ease of interconnection with the electricity grid. It is not, however, ideally suited for wind applications due to the high variability and unpredictability of wind energy. When the generator is in operation, if the torque generated by the wind suddenly becomes insufficient to maintain the synchronous speed, power must be drawn from the electricity grid in order for the generator to continue operating.

## Asynchronous (Induction) Generators



**a. stator**

**b. rotor**

**Fig. 6. Asynchronous Generator**

Although the induction generator is the most common choice for wind power applications, it is not widely used outside the wind turbine industry due to difficulty in interconnection. Because the power generated is not synchronized to the AC frequency of the electrical grid, interconnection requires that the output be converted to DC, then back to AC at the precise frequency of the grid.

## Hub

Most commercial turbines have a height of from 65 m to 156 m. Generally speaking, the hub height can be approximated as 1.3 times rotor diameter. The hub height for the selected locations was chosen to be 80m.

The hub generally is not a component that is prominently discussed in manufacturer literature and its scaling with rotor size does not command much discussion in research literature. The mass estimating approach used by GEC resulted in a hub-mass scaling relationship of [2]:

$$m = 0.24 \times D^{2.58} \quad (13)$$

In which, D is the rotor diameter. So, the hub mass of the designed wind turbine will be 19507 kg.

## Energy Storage

In a restructured power market, as Illinois is scheduled to become at the end of 2006, the Independent System Operator (ISO) performs day-ahead scheduling. Because generators each have different efficiencies and physical limitations, the ISO runs a Security Constrained Unit Commitment (SCUC) program one day in advance to schedule which generators will be turned on, and at what times, during the following day. The scheduling is based on the price of running the generators, so the cheapest generators, such as nuclear and large coal, are committed first, and more expensive gas units are only turned on during the middle of the day when the electricity demand peaks. Because more expensive units must be used during peak hours, the price of energy increases dramatically during this time, often three to five times the price at hours of low demand.

The power generated by wind turbines does not necessarily correlate to the peak energy price. In fact, wind is often stronger at night, when the energy demand is very low. Therefore, it is desirable to store the wind energy that is generated when the price of electricity is very low, and discharge it when the price is high. This is difficult to accomplish, as electrical energy can not be easily stored, so the electrical energy must be transferred to another form.

A sample daily energy price is shown below in Fig. 7. Based on the figure, the potential revenue without any energy storage is approximately 78% of the revenue with unlimited energy storage and selling only at the peak hour. Therefore, in order for it to be economical, the energy storage efficiency must be significantly greater than this value.

The three most common energy storage techniques are batteries, compressed air, and pump storage.

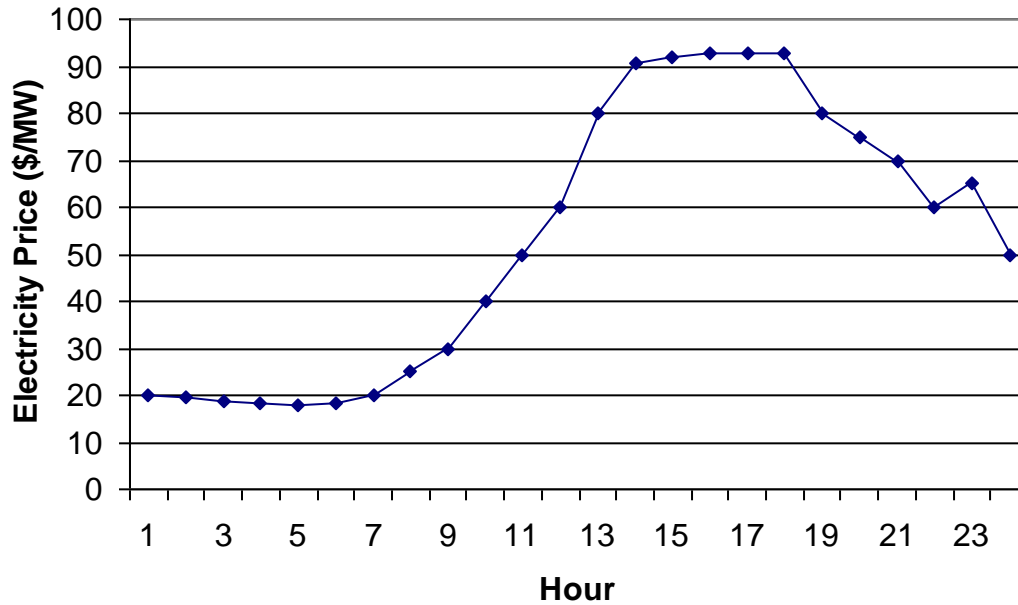


**Fig. 7. Sample Daily Electricity Price**

### Batteries

Battery storage is often the most efficient means to store electrical energy. If it is desired to store only 50% of the daily energy generation, the total storage capacity would need to be approximately  $2.5MW \cdot 24hours \cdot 50\% = 30,000kWh$ . Three of the largest commercially available batteries were evaluated, and the results are shown in Table IV. Based on these results, battery storage is simply impractical. Not only is the cost prohibitively high, but the physical space requirements for 500 to 1000 batteries makes them impractical.

**Table IV: Battery Parameters**

Name	Capacity	Price Each	Number Required	Total Cost
600AH	7.2 kWh	\$1,296	1,667	\$5,401,080
1275AH	27.3 kWh	\$2,275	440	\$2,502,500
1500AH	18 kWh	\$2,832	667	\$4,722,360

## **Compressed Air Energy Storage Systems**

Compressed Air Energy Storage (CAES) is a technology in which energy is stored in the form of compressed air in an underground cavern. Air is compressed during off-peak periods and then used on demand during peak periods to generate power with a turbo-generator system.

A typical CAES unit consists of five basic components:

1. Compressor train (compressor, inter-coolers and after-cooler);
2. Motor Generator;
3. Turbine expander train (including expanders and combustors);
4. Recuperator; and
5. Underground cavern

Electricity from the grid powers an electric motor, which drives an air compressor. The heat generated by the compression process is extracted by inter-stage cooling and after cooling and stored. Most of the electric energy from the grid is therefore stored as the pressure potential energy of the compressed air in the cavern, with the small amount extracted by the compressor coolers is stored as heat energy.

When air is extracted from the cavern, it is first preheated in the recuperator. The recuperator reuses the energy extracted by the compressor coolers.

An important performance parameter for a CAES system is the charging ratio, which is defined as the ratio of the electrical energy required to charge the system versus the electrical energy generated during discharge (the number of kWh input in charging to produce 1 kWh output). A low charging ratio results in low off-peak electrical energy requirements during the charging cycle.

Fast start-up is an advantage of CAES. A CAES plant can provide a start-up time of about 9 minutes for an emergency start, and about 12 minutes under normal conditions. By comparison, conventional combustion turbine peaking plants typically require 20 to 30 minutes for a normal start-up.

The first commercial scale CAES plant in the world is the 290MW Huntorf, Germany, plant operated by Nordwest Deutsche Kraftwerke (NDK) since 1978. The Huntorf plant runs on a daily cycle in which it charges the air storage for 8 hours and provides generation for 2 hours. The plant has reported high availability of 86% and a starting reliability of 98%. The Huntorf plant has a salt cavern.

The Alabama Electric Co-operative, Inc, in McIntosh, Alabama built the second commercial scale CAES plant. This plant has the maximum existing CAES cavern capacity of around 1.8 million cubic metres. It began operation in 1991 and provides 110 MW of power generation. The cavern for the McIntosh plant was mined from a salt dome by dissolving salt with fresh water. The cavern which is 70m in diameter, 305m tall and 460m below grade, supplies compressed air supporting generation of 100MW for 26 hours. The CAES plant has a full load net plant heat rate of 4819 kJ/kWh (74.7 % thermal efficiency) with a charging ratio of 1.3.

In addition to the NDK and the McIntosh CAES facilities, a 35MW CAES unit is under construction in Japan. Israel also has a 100MW CAES unit under construction, which uses an aquifer cavern for storage.

## Pump Storage

Pump storage units consist of a reservoir at high elevation and a second at low elevation. At times when the electricity price is very low, the power generated by the wind is used to pump water to the high elevation reservoir. Then, during hours of peak price, water is released into the low reservoir, running the pumps in reverse, and generating power to supply to the grid.

Traditionally, pump storage units use natural geographic features. For example, a high elevation lake could be created in a mountainous area to pump water when electricity prices are low. In order to generate electricity, it is necessary for the high elevation reservoir to be at least 100 meters above the low elevation reservoir. These elevation differences simply do not exist in Illinois. Several options exist, however. An underground reservoir, as shown in Fig. 8, could be created. Water would be released into it at peak hours, and pumped out at hours of excess generation.

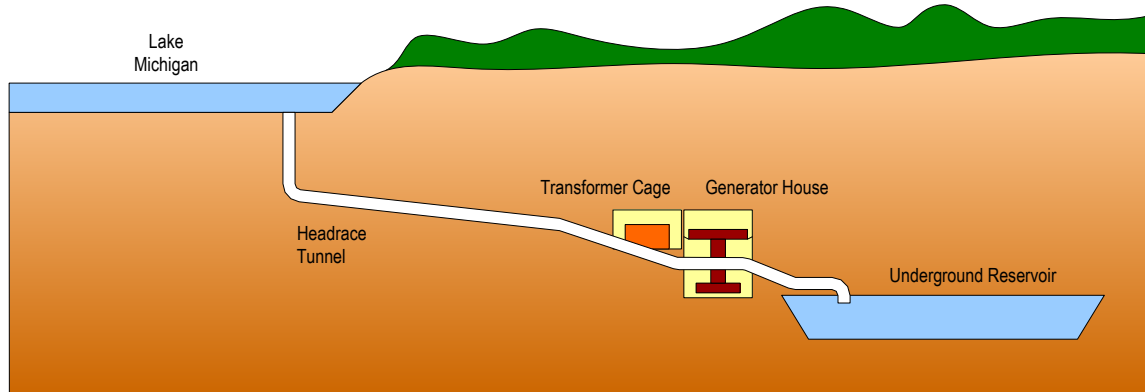


**Fig. 8. Proposed pump storage facility**

The rated power depends on the depth of the underground reservoir and can be calculated by

$$P = Q \times H \times \rho \times g \times \eta \quad (14)$$

where,

- P = Power transmitted to the pump by the water in (Watts)
- Q = Flow of water in tunnels ( $\text{m}^3/\text{s}$ )
- H = Elevation difference between the low and high reservoirs (m)
- g = Average Intensity of gravity (9.8 m/s)
- $\rho$  = Water density ( $1000 \text{ kg}/\text{m}^3$ )
- $\eta$  = Power Plant efficiency (95% to 97%)

## ***Economic Value***

Using the weather data, the RETScreen program [9] was used to study the net present value (NPV) and the number of years required to reach a positive cash flow.

Net present value is the primary method to measure the profitability of certain project. All the projects have cash flow in present and future, and the net present value would start with the concept of that today's money has more value than future's. In this sense, the net present value would discount the future cash flow at a rate which involves inflation, real interest rate, and risk. For example, today's \$100 has same value as the future's \$110 after 10% of inflation in the period. As a result, the net present value is to calculate the discounted difference between cash inflow and cash outflow for whole project time in present value. So, positive NPV values are an indicator of a potentially feasible project. The NPV was calculated based on the formula

$$NPV = \sum_{t=1}^T \frac{C_t}{(1+r)^t} - C_0 \quad (15)$$

where

$NPV$  = Net Present Value

$T$  = lifetime of the turbine, assumed to be 25 years

$t$  = year, from one to  $T$

$r$  = discount rate, assumed to be 12%

$C_t$  = cash flow at year  $t$

$C_0$  = initial investment

Additionally, the number of years to reach a positive cash flow was calculated. The year-to-positive cash flow considers project cash flows as well as the financial leverage (level of debt) of the project, which means that it measures the time to recover its own equity portion of project rather than whole initial cost of investment. So with 100% of debt ratio of the project (or no equity portion in the investment), the year-to-positive cash flow is immediate. And the year-to-positive cash flow is also a secondary indicator to analyze the risk.

None of the locations were profitable with only a single turbine in operation due to the high initial cost. For all but the Pittsfield site, however, increasing the number of turbines increased the NPV. For Pittsfield, the revenue generated never offset the operating costs, so the NPV actually decreased as more turbines were added.

Electricity rates are expected to increase dramatically at the end of 2006, however, a precise value is unknown. Shown below in Fig. 9 and Fig. 10 shows the net present value and the number of years to reach a positive cash flow for each of the four locations as a function of the number of wind turbines added at the proposed site as well as the selling price of electricity, ranging from five to eight cents per kilowatt hour.

Based on the above plots, the Chicago location remains the best, as the payback period is the shortest in all cases, however, this analysis does not take into account the increased cost of building offshore.

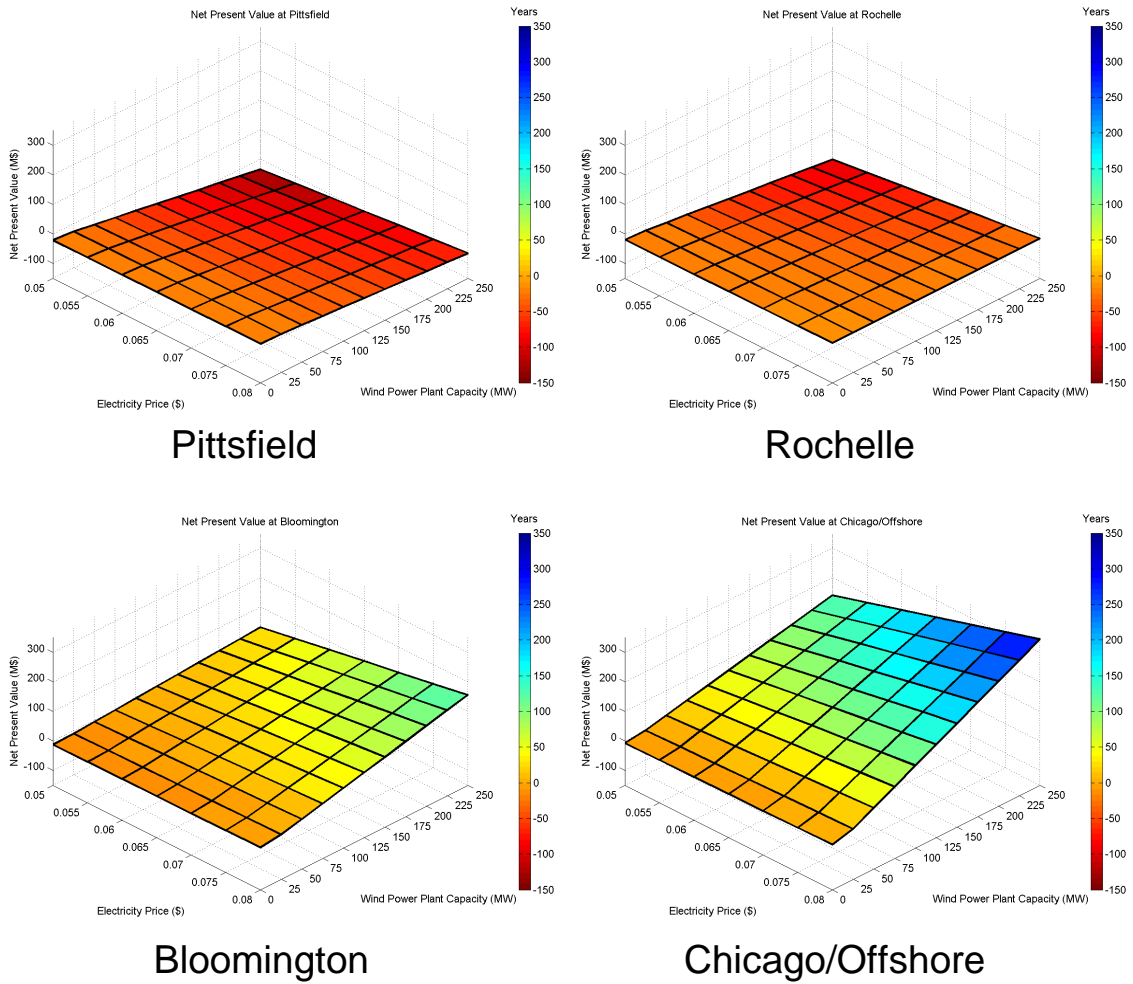


**Fig. 9. Net Present Value**

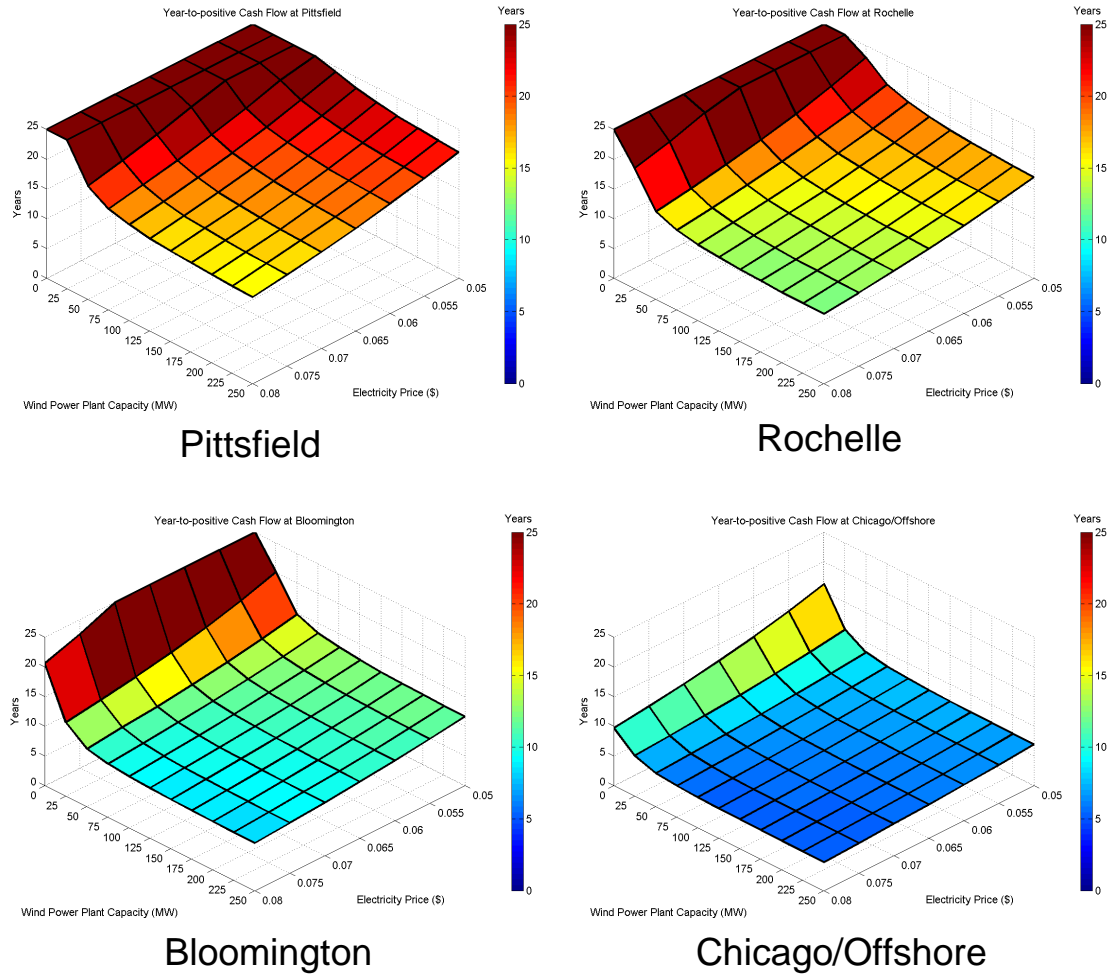


**Fig. 10. Years to positive cash flow**

## ***Power System Impact***

By using the energy storage to release the wind energy during the peak hours, it is believed that less of the more expensive peaking units will be necessary, and so the price of electricity at peak hours should decrease as more units are added.

In order to verify this assertion, the day-ahead scheduling program (SCUC) was run with actual data for the ComEd power system in the Chicago area. The Pittsfield location is not served by ComEd, and so it could not be included in these studies. Wind Turbines were connected at three different buses, as shown in Table V.

The daily unit commitment, power generation dispatch and electricity prices were simulated using an existing SCUC program developed by the Electric Power and Power

Electronics center at IIT. Figures 11 through 13 show the resulting energy price (LMP) as a function of the size of the wind farm. It is assumed that the rated capacity of a single turbine is 2.5 MW, so for a wind farm of 250 MW, for example, 100 turbines are required. As expected, the LMP did decrease as the number of turbines increased, however, the difference was not very significant. This is due to the fact that for the Chicago system, there are a large number of expensive generators that must be used. Increasing the wind capacity resulted in using less of these expensive generators, but the price did not decrease because expensive units were still required, and the price is set by the most expensive unit.

**Table V. Bus Locations**

Location	Bus ID	Substation Name	Bus Number
Chicago	36394	Taylor	261
Bloomington	37135	Powerton	251
Rochelle	37166	Steward	823

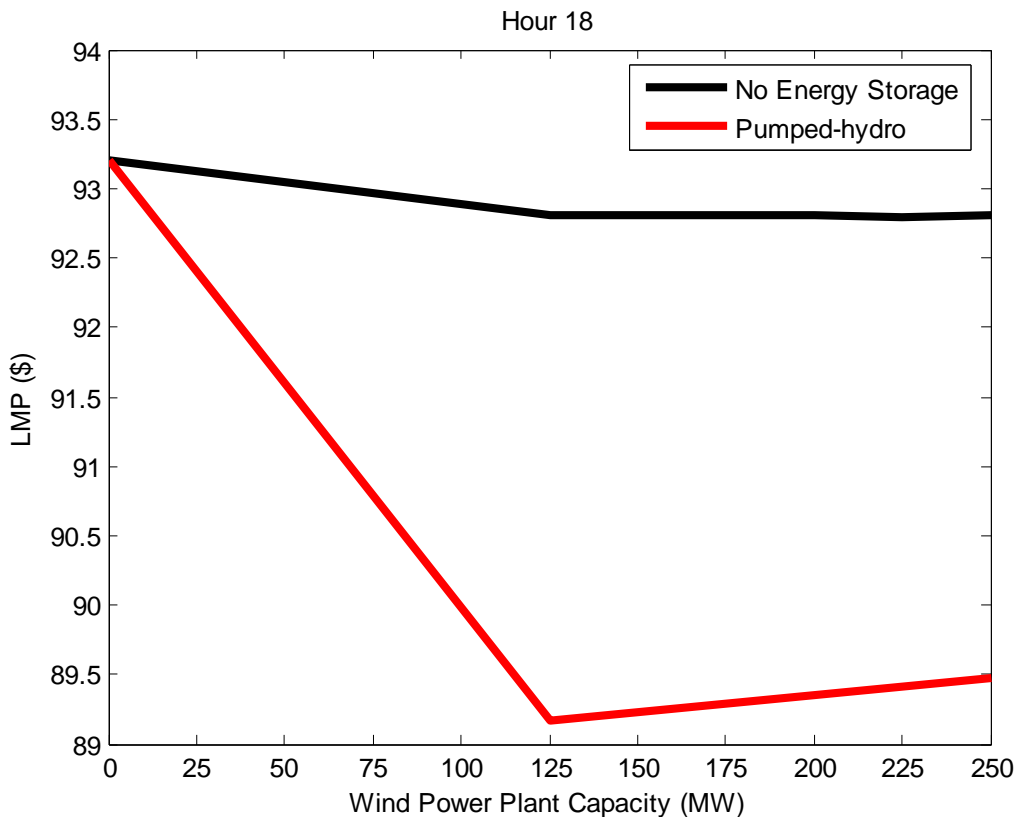


**Fig. 11. Energy Price at Chicago Location vs. Wind Farm Capacity**

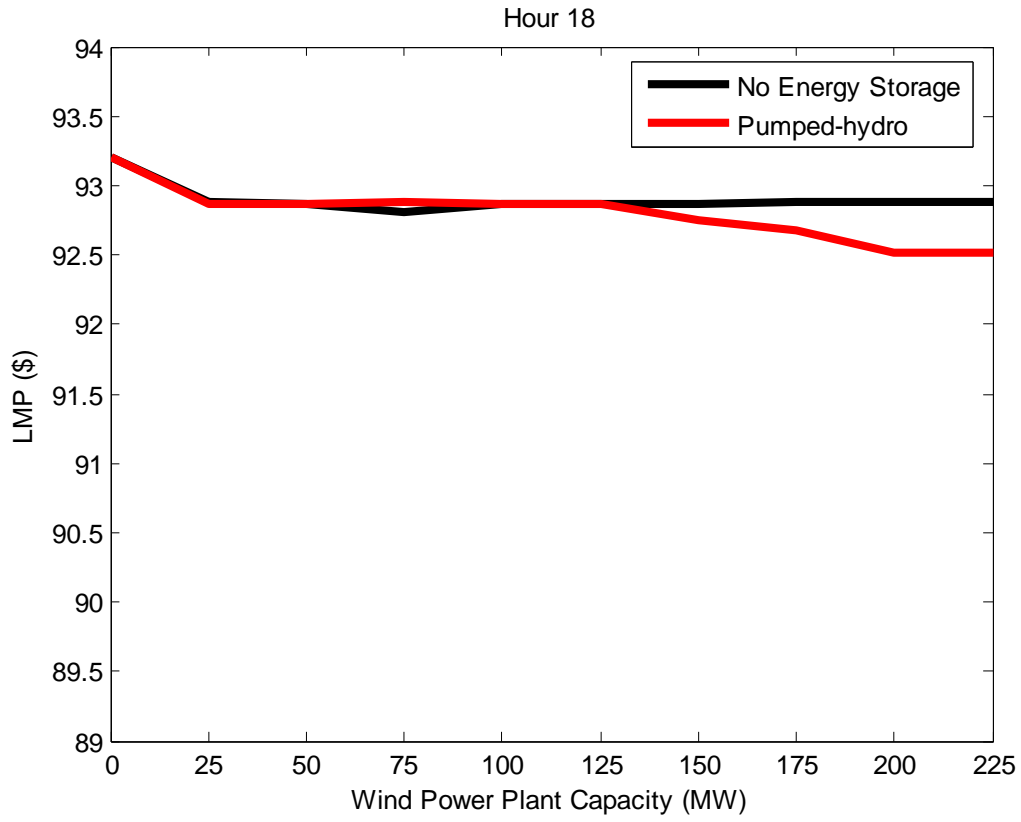


**Fig. 12. Energy Price at Bloominton Location vs. Wind Farm Capacity**

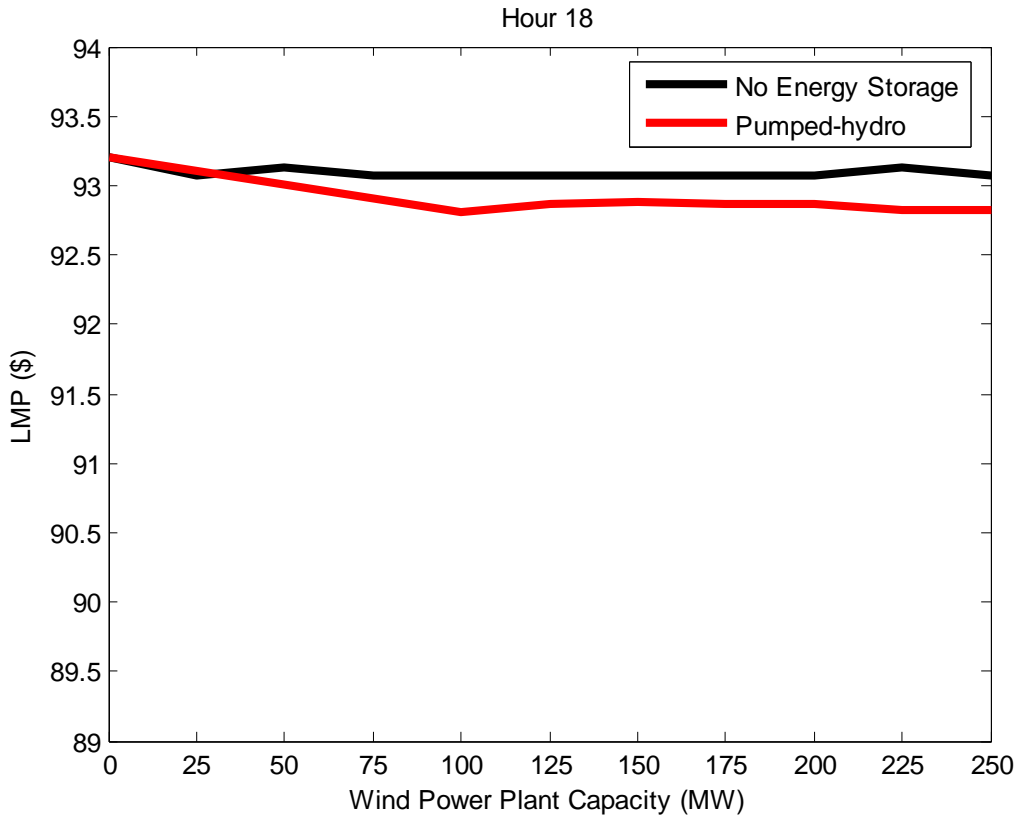


**Fig. 13. Energy Price at Rochelle Location vs. Wind Farm Capacity**

## ***Conclusion***

In the above report, the weather data for the Bloomington, Rochelle, Pittsfield, and offshore Chicago locations were summarized. Based on this data, a blade radius of approximately 45m was determined to be suitable for all locations. The energy output was calculated, and the economic feasibility of adding multiple turbines at each location was summarized. Based on this data, it was determined that the offshore Chicago location offered the highest, most consistent wind speeds. The added cost of building offshore, however, was not reflected in the analysis due to insufficient cost data.

## **Revised Task / Event Schedule / Task Assignments**

Currently, the schedule has deviated very little from the initial plan, however, the economic market analysis were given priority over the electrical design. Therefore, the electrical design was postponed. For a detailed breakdown of the timeline, please see the attached Gantt Chart.

# Barriers and Obstacles

## Market Analysis

By using the pump storage to release the wind energy during the peak hours, it is believed that less of the more expensive peaking units will be necessary, and so the price of electricity at peak hours should decrease as more units are added. In order to verify this assertion, a day-ahead scheduling program was run with actual data for the power system in Illinois. Due to security concerns, however, this data is no longer readily available to the public. The two Independent System Operators (ISO's) in Illinois, PJM in the Chicago area, and MISO in central and southern Illinois were contacted, however, they were unwilling to provide the data. ComEd, however, has provided some data to the Electric Power and Power Electronics Center (EPPEC) at IIT for a previous project. This data does include the physical data for the entire ComEd power transmission system, consisting of 1168 buses, however, it does not include the physical locations of the buses, so it could not be determined which buses the wind turbines should be connected to. Older maps of the system were provided by Professor Shahidehpour and Professor Fluek, which included some of the physical parameters of the lines. The bus locations could therefore be determined by matching the parameters of the lines on the map connected to the desired buses with the line parameters in the data files.

Three of the four locations to be studied, Bloomington, Rochelle, and the offshore Chicago location, were within the ComEd transmission system. The fourth location, Pittsfield, was not. This location, however, was economically the worst location. The wind speeds were not high enough to make any wind project profitable at this location, so it was decided to exclude the location from the market study.

An SCUC program which includes routines to schedule wind and pump storage units has been developed by EPPEC, and is readily available for use for the IPRO project. It was desired to run SCUC repeatedly to produce a plot, showing the number of wind turbines at a specific location vs. the resulting price of energy calculated by SCUC for the peak hour. To produce a reasonably accurate plot it was decided to run SCUC with zero to 100 turbines, in steps of 10, so for each location, SCUC must be run 11 times. Unfortunately, since the ComEd system is extremely large, the SCUC program could take up to 10 hours to run only once. To run all of the cases for just one location could then take over a week. It was observed, however, that with a difference of ten turbines, the SCUC solution may not change very much. Therefore, by using the solution from the previous run as the initial solution for the next run, the solution time was reduced dramatically. In some cases, it was less than two minutes to run a single case. The initial case for each location still took several hours, however, all subsequent cases executed in less than a half hour total.

## Weather Data

In order to determine the feasibility of a wind power project, very detailed data for wind speed, wind variability, and other measurements are necessary for the specific locations being studied. In industry, before a company chooses a final location, they would likely

place their own equipment on a prospective site to gather weather data for an entire year. Clearly this option is not available for the purposes of the IPRO project. Therefore, it was necessary to obtain publicly available data from the National Oceanic and Atmospheric Administration for observation sites nearby our locations. For the Pittsfield, Bloomington, and offshore Chicago locations, weather observation stations were located reasonably nearby. For the Rochelle location, however, there were no observation stations anywhere within the area designated by the DOE wind resource map as having good wind potential. It was necessary to use data from the nearest observation station, which was more than twenty miles from the Rochelle location. It is believed that the wind speeds at the actual location would be at least as good, if not better than the wind at the observation station.

### **Costs of turbines**

In studying the profitability of the wind project, ideally, the actual costs of installing a turbine must be known. Manufacturers of wind turbines do not publish this data, and are unwilling to produce a price estimate for students. Additionally, the costs of development, installation, operation, and maintenance were not available. Some average costs were published by the Canadian government, and these were used.

## **References**

- [1] U.S. Department of Energy (DOE), “Wind Powering America: Illinois Wind Maps”, Energy Efficiency and Renewable Energy (EERE), 2006, [On-line], Available at: <http://www.eere.energy.gov/windandhydro/>, Accessed on 10/05/06.
- [2] National Oceanic & Atmospheric Administration (NOAA), “Past Weather Data”, National Environmental Satellite, Data, and Information (NESDIS), 2006, [On-line] Available at: <http://www.ncdc.noaa.gov/oa/ncdc.html>, Accessed on 10/05/06.
- [3] Danish Wind Energy Association (DWEA), “Guided Tour on Wind Energy: Wind Energy Manual”, 2006, [On-line], Available at: <http://www.windpower.org/>, Accessed on 10/05/06.
- [4] “Air Density and Density Altitude Calculations”, [On-line], Available at: [http://wahiduddin.net/calc/density\\_altitude.htm](http://wahiduddin.net/calc/density_altitude.htm), Accessed on 10/10/06.
- [5] “RETScreen International Clean Energy Project Analysis Software: Wind Energy”, [On-line], Available at: <http://www.retscreen.net>, Accessed on 09/23/06.
- [6] S. Mathew, “Wind Energy: Fundamentals, Resource Analysis and Economics”, Springer, Netherlands, 2006
- [7] R. Harrison, E. Hau, H. Snel, “Large Wind Turbines: Design and Economics”, John Wiley & Sons, 2001
- [8] Kevin Smith, “WindPACT Turbine Design, Scaling Studies Technical Area 2: Turbine, Rotor, and Blade Logistics”, Global Energy Concepts LLC, Kirkland, Washington,, March 27, 2000 to December 31, 2000.
- [9] “Journal of Hydrology” , New Zealand Hydrological Society, 2005.